Check for updates

Improving the clinical workflow of a MR-Linac by dosimetric evaluation of synthetic CT

Bin Tang[1,2], Min Liu[1], Bingjie Wang[3], Peng Diao[1]*, Jie Li[1],
Xi Feng[1], Fan Wu[1], Xinghong Yao[1], Xiongfei Liao[1], Qing Hou[2]
and Lucia Clara Orlandini[1]

[1]Department of Radiation Oncology, Sichuan Cancer Hospital and Research Institute, affiliated to
University of Electronic Science and Technology of China (UESTC), Chengdu, China, [2]Key
Laboratory of Radiation Physics and Technology of the Ministry of Education, Institute of Nuclear
Science and Technology, Sichuan University, Chengdu, China, [3]Faculty of Arts and Science,
University of Toronto, Toronto, ON, Canada

Adaptive radiotherapy performed on the daily magnetic resonance imaging
(MRI) is an option to improve the treatment quality. In the adapt-to-shape
workflow of 1.5-T MR-Linac, the contours of structures are adjusted on the
basis of patient daily MRI, and the adapted plan is recalculated on the MRI-
based synthetic computed tomography (syCT) generated by bulk density
assignment. Because dosimetric accuracy of this strategy is a priority and
requires evaluation, this study aims to explore the usefulness of adding an
assessment of dosimetric errors associated with recalculation on syCT to the
clinical workflow. Sixty-one patients, with various tumor sites, treated using a
1.5-T MR-Linac were included in this study. In Monaco V5.4, the target and
organs at risk (OARs) were contoured, and a reference CT plan that contains
information about the outlined contours, their average electron density (ED),
and the priority of ED assignment was generated. To evaluate the dosimetric
error of syCT caused by the inherent approximation within bulk density
assignment, the reference CT plan was recalculated on the syCT obtained
from the reference CT by forcing all contoured structures to their mean ED
defined on the reference plan. The dose−volume histogram (DVH) and dose
distribution of the CT and syCT plan were compared. The causes of dosimetric
discrepancies were investigated, and the reference plan was reworked to
minimize errors if needed. For 54 patients, gamma analysis of the dose
distribution on syCT and CT show a median pass rate of 99.7% and 98.5%
with the criteria of 3%/3 mm and 2%/2 mm, respectively. DVH difference of
targets and OARs remained less than 1.5% or 1 Gy. For the remaining patients,
factors (i.e., inappropriate ED assignments) influenced the dosimetric
agreement of the syCT vs. CT reference DVH by up to 21%. The causes of
the errors were promptly identified, and the DVH dosimetry was realigned
except for two lung treatments for which a significant discrepancy remained.
The recalculation on the syCT obtained from the planning CT is a powerful tool
to assess and decrease the minimal error committed during the adaptive plan
on the MRI-based syCT.

Introduction

The roles of image guidance, adaptive planning, and magnetic resonance imaging (MRI) in radiation therapy have been increasing over the last two decades. Several authors have recently demonstrated that the possibility to modify the radiation treatment according to the patient's daily anatomy (1) can effectively manage the inter-fraction variation in OAR and target position and shape that adversely affect treatment accuracy and patient outcomes (2, 3). Most recently, magnetic resonance (MR)–guided radiation therapy (MRgRT) has provided the opportunity for fractional online adaptive radiotherapy (ART) for patients undergoing radiation therapy (4). The hybrid RT machines, combining a MR scanner with a RT delivery system, enable soft tissue contrast daily MRI to visualize all anatomical changes during the course of radiotherapy (5–7); subsequently, the adaptive planning taking into account changes in target/OAR shape and position can be performed.

Several centers presented the feasibility and clinical advantages of using MR-Linear accelerator (MR-Linac) machines for the treatment of tumors located in different sites, and this method is becoming increasingly popular (1, 7–10). Although this clear clinical advantage, there are approximations in the procedure, i.e., the assignment of CT-based electron density (ED) values to structures in the MR image data set, that should be investigated by the user to ensure the quality of the treatment performed (11). Because of the lack of tissue density information needed for dose calculation in MRgRT, an ED map was generated from MRI to allow for adaptive planning based on daily MRI. To address this issue, several approaches have been developed to generate ED maps also called synthetic computed tomography (syCT) from MRI (MRI-based syCT): i) the bulk density assignment (12–19) consisting in a direct density assignment methods that determine volumes of interest (tissues or organs) on the patient's MRI and assign them a given density; ii) atlas-based method (20–22) based on atlas registration that spatially map an image (for example, CT) to the patient's MRI, merging them to generate a pseudo CT scan; and iii) voxel-by-voxel conversion (23–27) and deep learning (28–40) are based on statistical learning model relationships between CT and MRI intensities and then apply the resulting model to the patient's MRI. As an emerging method, deep learning indeed shows promising results, reflecting in high accuracy, automation, and efficiency in the

generation of syCT from MRI. However, there are still some obstacles to be overcome before deep learning–based methods can be implemented, for example, most of those studies are anatomical site-specific, MRI sequence–specific, lack of external validation, etc. Bulk density assignment is a straightforward way to generate syCT. As the simplest way of bulk assignment, assigning the whole patient volume to a single homogeneous media could produce a relative large dose error (> 2%) (15, 41); more sophisticated ways, such as separating the tissues in MRI into several classes and then assigning an ED to each class, show clinically acceptable error (around 1%) (17, 42). Previous studies (43, 44) also reveal the concerns regarding the impact of density inhomogeneity on patient dosimetry in the presence of a magnetic field. The strategy of syCT applied in Monaco (Elekta AB, Stockholm, Sweden) treatment planning system (TPS) for 1.5-T MRgRT is the bulk density assignment based on the contours drawn on patient simulation CT. More specifically, during the online adapt-to-shape (ATS) procedure, the daily acquired MRI will be deformably registered to simulation CT, then all contours information including average ED and the priority of density assignment on CT are propagated to MRI, and then syCT is generated by the bulk density assignment on MRI. It is well known that contouring is a critical step in the radiotherapy process (45); the quality of the initial contours can have significant effect on the therapeutic ratio, and several studies have linked contouring protocol deviations with decreased survival and increased toxicity (46). In the case of adapted plans recalculated on syCTs generated by the bulk density assignment of the contours, contouring has a much greater weight as it also impacts on the accuracy of the calculation itself. Considering that the adapted plan is reoptimized and recalculated on the syCT, the dosimetric accuracy of this strategy is a priority and requires evaluation (47–49). In this article, on the basis of our clinical experience, we propose the addition of a simple procedure into the clinical routine to ensure that the dosimetric error of syCT generated by the bulk density assignment remains small.

Materials and methods

Patients

Sixty-one patients consecutively treated at 1.5-T MR-Linac (Unity, Elekta, Crawley, UK) were included in this study.

Patients who had different tumor sites were treated with different prescription doses and referring physicians. All patients provided informed oral consent at the use of their clinical data for research purposes. The study was approved by the institutional ethics Committee (SCCHEC-02-2022-003).

CT and MR simulation

Patients were set up in the supine position using indexed patient positioning aids; with the exception of brain treatments and the first two rectum patients for which thermoplastic masks were used, all patients were immobilized using Wing-STEP, KneeSTEP, and FeetSTEP supports (IT-V, Innsbruck, Austria). Patients underwent a three-dimensional (3D) or four-dimensional (4D) (lung and liver cases) CT scans; a first non-contrast CT series used for the treatment planning was acquired, followed by one with the contrast used as support for the physician in the tumor delineation; in addition, T2-weigthed simulation scans on the 1.5-T MR-Linac were acquired immediately after CT simulation in the same position and with the same immobilization devices. Patients with liver and kidney disease were asked to wear a containment belt to reduce the respiratory movement, reducing artifacts as well at the simulation and delivery session. Considering the dosimetric challenge that can result from inconsistent bladder filling between simulation and delivery (50), patients with disease of the rectum, prostate, and cervix treated, prior to CT and MRI simulation scans and then prior to each MRI performed on the day of treatment (upon patient arrival and after approval of the treatment plan prior to beam delivery), were fitted with a bladder catheter to ensure the same bladder filling between the daily MR scan and treatment delivery.

Delineation and planning on reference CT

The delineation of targets and OARs and the reference treatment planning were performed in Monaco V5.4. The referring physician of each patient contoured on non-contrast CT but with the use of available imaging studies. For moving targets, the motion of the tumor was determined using information from 4D-CT; for liver and lung cases, an internal target volume was created under consideration of the maximum intensity projection (MIP) and minimum intensity projection, generated by reconstructing 10 respiratory phases. A reference plan was then optimized to achieve clinical goals using eight to 12 individual beam angles, 3-mm dose grid, and 1% calculation uncertainty.

Daily online ART

Daily Online ART was delivered in one of the two available procedures conventionally called ATP (adapt to position) and ATS (5). In both modalities, once the patient is positioned on the couch, an MRI is acquired then rigidly registered to the CT images of the reference plan. At this point, the plan can be adapted, i.e., optimized and recalculated on the reference CT images and contours accordingly to the patient positioning error determined by the image registration; this is the ATP workflow. On the other hand, the ATS workflow will be performed if there is still a large residual error although rigid registration has been applied, mainly because the shape or/and position of certain organ changes compared to when the reference CT was acquired. In ATS workflow, adjusting of contours according to daily MRI is needed, which is one of the most time-consuming (51, 52) steps; therefore, considering that there may be a significant time interval between the acquisition of the first daily MRI and beam delivery, our center while approving the adapted plan performs a second MRI that is rigidly registered with the one performed at the beginning of the session and on which the plan was adapted, to ensure the appropriateness of the ongoing delivered treatment. In case of position differences, a next step is performed, adjusting the isocenter position and recalculating the dose according to the ATP procedure.

Patient-specific QA

Treatment plan verifications were performed by comparing the x-ray fluence measured by a 3D dosimetry array (ArcCHECK®-MR, Sun Nuclear Corp., Melbourne, FL) with that computed by the TPS, for the reference plan and each adapted plan. The global gamma analysis with percentage signal to agreement and distance to agreement of the criteria of 3%/3mm was used for evaluation. The verification of the reference CT plan was performed before the start of the treatment course, whereas the online adapted plans based on the reference CT plan were verified (as only option for the nature of the clinical workflow) after their delivery to check the adequacy of the already administered treatment.

Dosimetric evaluation of synthetic CT

The clinical workflow was extended by adding extra steps between treatment planning on the reference CT and daily ART, as shown in Figure 1. The ready-to-use reference CT plan in the ATS workflow contains all the density bulk assignment information, i.e., the contours, their corresponding average ED, and the priority of each contour concerning density

FIGURE 1
Clinical workflow integrated with quality control on dosimetric accuracy of synthetic CT plan.
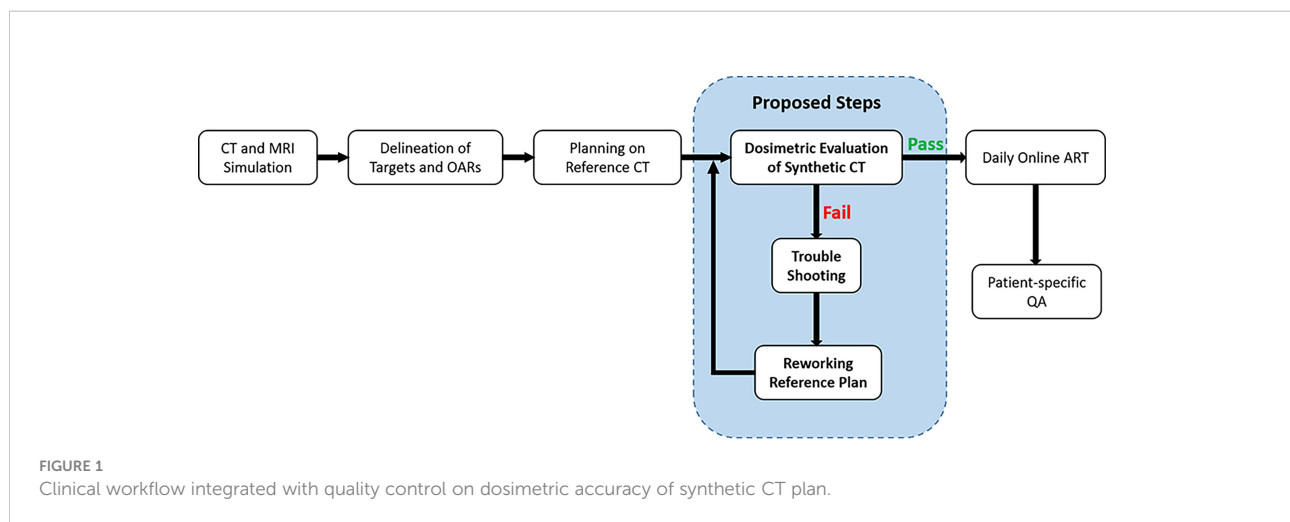
assignment in case of contour overlaps. The reimaging of a specific district of a patient does not result in perfectly superimposable images, as organ profiles and/or their relative positions are influenced by many factors such as bladder and/or rectum filling, gas in the intestines, and contouring. Therefore, to assess the dosimetric error of plan recalculation on syCT caused by the loss of density inhomogeneity during the ATS procedure and to exclude other potential factors affecting the results of the calculation (i.e., recontouring on daily MRI), for each patient, the "ideal" syCT is generated using the reference CT imaging, contours and EDs, and the priorities indicated in the reference plan; then, the reference CT plan is recalculated (not reoptimized) on the generated syCT. Then, targets and organs at risk (OARs) dose–volume histogram (DVH) of the CT and syCT plans as well as the dose distributions using gamma analysis with the criteria of 3%/3 mm and 2%2 mm were compared. The DVHs and corresponding dosimetric parameters of the CT and syCT treatment plans were obtained directly from Monaco TPS. The volume of the target covered by the prescription dose (V_{Dpre}) and the clinically concerned OAR dosimetric parameters with the corresponding constraints were compared from the DVHs. DICOM-RT files including CT images, RT plans, RT structures, and RT dose were exported to MATLAB R2013a; 3D gamma analysis between dose of CT and syCT was performed by CERR v4.4 (https://github.com/cerr/CERR). Treatment plan calculation was considered in agreement when the percentage of points with $\gamma < 1$ is higher than 99% with the criteria of 3%/3 mm and the target dose difference in any point of the DVH is lower than 1.5% or 1 Gy.

Trouble shooting and reworking of reference plan

Dose discrepancy could be detected by the comparison of CT vs. syCT DVHs and/or the gamma analysis. The causes were then investigated by several means, including a preliminary visual comparison of the syCT vs. CT and its contours, spotting abnormalities in ED values assignment to the various contours, checking priority assigned in case of their overlap in the treatment plan, focusing on the organs/regions with the greatest deviations, etc.

After the corresponding corrections were made in the reference plan, a new syCT was generated, and the plan was recalculated on the new syCT. Then, the dosimetry of the two plans was compared again. If the causes were not obvious or the dosimetric difference persists, then the discrepancy was notified to the radiation oncologists for their clinical decision regarding treatment delivery.

Results

The clinical characteristics of the patients and the treatment schedule followed are shown in Table 1. Included patient samples were 57.4% of men and 42.6% of women, with a median age of 58 years at the time of radiotherapy; among the investigated treatment sites, the liver was the most common with 21 patients treated, followed by cervix and rectum with 12 and seven cases, respectively; 77.0% of patients followed the ATS workflow and the remainder the ATP workflow.

A total of 475 reference and adaptive plan verifications were performed with ArcCHECK. The results of gamma analysis with the criteria of 3%/3 mm for different tumor sites showed high accuracy with a median pass rate of 98.2% (range, 92.3%–100.0%); the details were shown in Table 2.

The procedure to generate a syCT from the original reference CT and, subsequently, to recalculate the plan on the syCT took an average time of 312 s (minimum, 253 s; maximum, 400 s); it is therefore feasible within the clinical workflow. The dosimetry of the reference CT plan was consistent with the corresponding dosimetry on the syCT for 54 of the 61 patients:

TABLE 1 Patient characteristics, tumor site, and adopted treatment schedule.

	N°	Age year median (range)	Sex no. M-F	BMI kg/m² median (range)	Dose Gy range	Dose/fr Gy/fr range	Schedule no. ATS-ATP
Rectum	7	50 (45–63)	6–1	23.5 (19.0–29.7)	25	5	7–0
Cervix	12	55 (44–66)	0–12	25.9 (20.8–29.4)	10–25	5	12–0
Lung	2	64 (58–70)	2–0	21.4 (19.8–23.1)	42–48	6–8	0–2
Prostate	3	71.5 (60–83)	3–0	22.2 (19.5–24.9)	56	2.8	3–0
Kidney	4	58 (58–69)	3–1	21.5 (20.9–24.2)	36–50	5–8	3–1
Pancreas	6	62 (48–78)	3–3	23.9 (20.8–25.4)	36–48	6–8	2–4
Liver	21	52 (41–75)	14–7	22.7 (16.4–25)	24–50	6–15	16–5
Brain	6	57 (31–68)	4–2	21.7 (16.4–26.7)	36–50	5–8	4–2
Total	61	58 (31–5)	35–26	23.4 (16.4–29.4)	10–50	5–15	47–14

BMI, body mass index; ATP, adapt to position; ATS, adapt to shape.

The absolute difference of the target and OARs DVH dosimetric parameters remained below 1.5% for ∇Vx . (percentage of volume receiving × Gy) and lower than 1 Gy for ∇Dy . (dose in Gy received by the volume y), respectively, as reported in Table 3; similarly, the results of the dose distribution comparison performed on the whole volume, targets, and OARs by the 3D gamma analysis with the criteria of 3%/3 mm and 2%/2 mm were 99.7% and 96.3%, respectively, confirming the agreement found with the DVHs comparison. The details of the results obtained are shown in Table 4.

Seven patients (two lung, two liver, two rectum, and one brain treatments, respectively) presented a discrepancy between CT and syCT target and/or OARs DVH dosimetry as well as lower gamma pass rate. Details of the dosimetric differences and gamma analysis obtained at first screening and after a rework of the reference plan are shown in Tables 5, 6, 7.

Large dosimetric discrepancies were recorded for both patients with lung cancer with target V_{Dpre} . = 6.1% and 18.6% for cases 1 and 2, respectively, persisting even after plan optimization (V_{Dpre} . = 6.2% and 17.9%, respectively). Because of the high ED gradient within the target, and between the target and the remaining part of the lung, the

assignment of an average ED was not able to accurately reproduce the dose calculation. Figure 2 shows the successive unsuccessful attempts made for lung case 1 to decrease the dosimetry discrepancy between syCT and reference CT plan. In the original plan, an average ED was assigned to the whole target drawn by the physician, as can be seen in the corresponding syCT (Figure 2B); then, the inhomogeneous density of the target was considered with a precise contour of relative high-density parts (Figure 2C); in the last attempt, the bones intercepting the beams entry were drawn (Figure 2D). Although there was an improvement in the target gamma analysis, the dosimetric difference was not reduced (Figure 2E), and the patient treatment proceeded using the ATP workflow. For lung case 2, the contours were set with appropriate ED in the original CT plan, and subsequent attempts did not lead to improvements; similarly, the patient was treated according to ATP workflow.

For the liver, rectum, and brain treatments, once the source of the errors was identified and corrected, the newly revised CT plan did not differ from its corresponding syCT.

Rectum case 1, the first rectum treatment scheduled at MR-Linac, was immobilized with a thermoplastic mask clamped to the patient positioning system (pps) plate as for standard Linacs.

TABLE 2 Quality assurance of treatment plans with ArcCheck: results of gamma analysis of reference and adapted plans.

	Pts no.	Reference plan no.	Adapted plan no.	3%/3 mm (%) median (range)
Rectum	7	7	35	99.2 (95.6–100.0)
Cervix	12	12	43	97.6 (92.3–100.0)
Lung	2	2	13	98.3 (95.2–100.0)
Prostate	3	3	60	97.5 (93.3–100.0)
Kidney	4	4	31	97.2 (95.7–99.6)
Pancreas	6	6	36	97.6 (93.0–100.0)
Liver	21	21	154	98.8 (93.2–100.0)
Brain	6	6	42	97.0 (92.9–100.0)
Total	61	61	414	98.2 (92.3–100.0)

TABLE 3   Absolute difference of CT vs. syCT targets and OARs DVH dosimetric parameters (mean and standard deviations) for 54 out of 61 patients, resulting in tolerance at the first CT vs. syCT plan comparison.

Site (no.)	CT vs. SyCT absolute dosimetric difference for targets and OARs						
Rectum (5)	*PTV*	*Bladder*		*Small Bowel*		*Colon*	*Fem Heads*
	V_{Dpre} (%)	$D_{0.5cc}$ (Gy)	D_{10cc} (%)	$D_{0.5cc}$ (Gy)	D_{5cc} (Gy)	$D_{0.5cc}$ (Gy)	D_{max} (y)	D_{10cc} (Gy)
	0.27 ± 0.33	0.17 ± 0.06	0.09 ± 0.13	0.30 ± 0.23	0.32 ± 0.38	0.35 ± 0.34	0.59 ± 0.28	0.06 ± 0.09
Prostate (3)	*PTVs*	*Bladder*		*Rectum*	*Rectum*	*Urethra*	*Fem. Heads*	*Sigmoid*
	V_{Dpre} (%)	$D_{15\%}$ (Gy)	$D_{60\%}$ (Gy)	$D_{15\%}$ (Gy)	$D_{60\%}$ (Gy)	D_{max} (Gy)	$D_{50\%}$(Gy)	D_{2cc} (Gy)
	0.60 ± 0.53	0.32 ± 0.47	0.05 ± 0.05	0.05 ± 0.01	0.04 ± 0.04	0.05 ± 0.02	0.01 ± 0.01	0.41 ± 0.47
Cervix (12)	*PTVs*	*Bladder*		*Rectum*		*Intestine*	*Fem Heads*	
	V_{Dpre} (%)	D_{1cc} (Gy)	D_{2cc} (Gy)	D_{1cc} (Gy)	D_{2cc} (Gy)	D_{2cc} (Gy)	V_{10Gy} (%)	Dmax
	0.40 ± 0.33	0.08 ± 0.05	0.05 ± 0.05	0.12 ± 0.18	0.25 ± 0.29	0.13 ± 0.11	0.04 ± 0.03	0.16 ± 0.21
Pancreas (5)	*PTVs*	*Spinal cord*	*Intestine*	*Liver*		*Pancreas-PTV*	*Kidney*	Stomach
	V_{Dpre} (%)	D_{max} (Gy)	D_{1cc} (Gy)	V_{20Gy} (%)	V_{5Gy} (%)	$D_{33\%}$ (Gy)	$D_{20\%}$ (Gy)	D_{1cc} (Gy)
	0.37 ± 0.39	0.15 ± 0.5	0.09 ± 0.08	0.13 ± 0.24	0.17 ± 0.31	0.04 ± 0.05	0.01 ± 0.01	0.06 ± 0.09
Liver (19)	*PTVs*	*Spinal cord*	*Duodenum*	*Liver -GTV*		Small bowel	Kidney	Bladder
	V_{Dpre} (%)	D_{max} (Gy)	D_{1cc} (Gy)	D_{mean} (Gy)	V_{5Gy} (%)	$D_{0.5cc}$ (Gy)	D_{mean} (Gy)	D_{1cc} (Gy)
	0.44 ± 0.76	0.05 ± 0.34	0.06 ± 0.06	0.01 ± 0.04	0.02 ± 0.08	0.07 ± 0.01	0.02 ± 0.04	0.13 ± 0.10
Kidney (4)	*PTVs*	*Spinal cord*	Intestine	*Liver*	*Kidney-GTV*		*Kidney cL*	*Pancreas*
	V_{Dpre} (%)	D_{max} (Gy)	D_{1cc} (Gy)	V_{5Gy} (%)	V_{10Gy} (%)	D_{max} (Gy)	D_{max} (Gy)	D_{max} (Gy)
	0.66 ± 0.39	0.05 ± 0.01	0.20 ± 0.13	0.09 ± 0.11	0.19 ± 0.45	0.10 ± 0.12	0.11 ± 0.06	0.60 ± 0.54
Brain (5)	*PTVs*	*Brain stem*		*Lens*	*Brain*	*Eyes*	*Opt.Chiasm*	*Opt. nerves*
	V_{Dpre} (%)	D_{max} (Gy)	$D_{50\%}$ (Gy)	D_{max} (Gy)	D_{mean} (Gy)	D_{max} (Gy)	D_{max} (Gy)	D_{max} (Gy)
	0.61 ± 0.73	0.01 ± 0.22	0.02 ± 0.03	0.03 ± 0.04	0.06 ± 0.08	0.10 ± 0.09	0.06 ± 0.06	0.06 ± 0.06

The isodoses of the reference CT plan differed significantly from the corresponding ones of syCT; moreover, no dose was visible within pps plate in the CT, whereas it was displayed on syCT. Further investigation established that, for the pps to be included in the TPS calculation, it is necessary to add such a region in the within the optimisation parameters. After reworking the reference plan, the doses obtained on syCT matched the doses calculated on the reference CT plan, as shown by the DVHs in Figure 3. For the rectum case 2, we observed an inappropriate setting in the layer prioritization of the parts of the pps plate with different ED, which was also corrected to achieve an agreement between CT and syCT dosimetry.

Regarding the CT and syCT dose discrepancy of the brain treatment, in the original CT plan, the region of interest (ROI) of the whole brain was given priority in ED allocation over other ROIs, resulting in the loss of skull on the syCT and leading to an unavoidable dosimetric difference. For the two liver cases, the lung and target contours drawn on the MIP CT did not match the organs on the reference CT, thus generating an incorrect ED

assignment on the syCT and leading to an understandable dose difference in both DVH dosimetry and gamma analysis. Figure 4 shows, for liver case 1, the gamma analysis results between the dose distribution of CT and syCT in transverse plane, before and after the original CT plan reworking, and corresponding DVHs.

Discussion

The use of MRgRT has raised the quality of all those treatments for which soft tissue visualization is essential, particularly suitable for precision treatments when the targets are close to risky structures and even more when high fractional doses are to be delivered (4, 7, 9, 53, 54). MRgRT performed with the Unity Linac allows through the ATS workflow to recalculate and reoptimize the plan using a syCT generated from the daily MRI. It remains therefore a crucial point to put in place all possible actions to ensure the accuracy of the calculation on this MR-based syCT (49).

TABLE 4   Median values and range of gamma analysis results performed comparing the dose distribution on CT to syCT for 54 patients with good agreement at the first check of the CT vs. syCT DVHs dosimetric parameters.

		Body (n = 54)	Targets (n = 69)	OARs (n = 270)
Gamma analysis	**3%/3 mm** (%)	99.7(99.0–100.0)	100.0 (98.4–100.0)	100.0 (83.4–100.0)
	2%/2 mm (%)	98.5 (95.7–99.8)	96.3 (84.7–100.0)	99.9 (78.1–100)

TABLE 5   Absolute difference of target and OARs DVH dosimetric parameters of the original CT and of the reworked CT vs. the corresponding syCT plans.

		PTV		Omolateral Lung		Body	
		Original	Reworked	Original	Reworked	Original	Reworked
Lung Case 1	ΔV_{Dpre} (%)	6.1	6.2	–	–	–	–
	ΔV5Gy (%)		–	1.1	1.1	–	–
	γ (3%/3 mm) (%)	40.7	62.4	86.1	87.4	93.2	93.9
	γ (2%/2 mm) (%)	19.6	33.5	64.5	65.5	82.4	82.4
Lung Case 2	ΔV_{Dpre} (%)	18.6	17.9	–	–	–	–
	ΔV5Gy (%)	–	–	0.7	0.7	–	–
	γ (3%/3 mm) (%)	59.9	59.1	100.0	100.0	98.8	98.8
	γ (2%/2 mm) (%)	31.2	30.1	84.4	85.0	94.9	95.0

OARs not reported in the table presented CT vs. syCT absolute difference of DVHs dosimetric parameters< 1 Gy or 1.5%, and a gamma analysis with 3%/3 mm and 2%/2 mm > 99.0% and 95.0%, respectively.

We have included in the clinical workflow a procedure to assess, for each individual treatment plan, the minimum error that we should expect when performing the recalculation on the syCT in the ATS procedure. The procedure consists of generating an ideal syCT using the reference CT and the information included in the reference CT plan, recalculating the original plan on the syCT, and comparing the dosimetry of the original CT and syCT with the DVHs. It is therefore a very intuitive procedure, easy to perform, and with short execution times; for the purpose of the research work, we added the gamma analysis evaluation, which gives further confirmation of the agreement/disagreement between the two dose distributions.

The results were satisfactory for most of the patients (54 out of 61). For the patients who had a syCT plan discordant with the original CT plan, the procedure allowed us to highlight the following: i) incorrect information or input given to the patient's treatment plan—treatment plan that was then reworked before its clinical use; ii) errors in the clinical workflow—revised and optimized; and iii) discrepancies related to tumor morphology/ location not manageable by the system—patients treated using another procedure. It is important to point out that these errors could not have been detected by the pre-treatment checks or at the plan adaptation phase. Moreover, the well-known criticalities in the treatment of targets in areas of high inhomogeneity (lung targets) can be quantified in a very simple way through the discordance of DVHs.

One of the criticisms of the ATS procedure is certainly the fact that the contours on simulation CT are automatically propagated by deformable registration onto the online planning MRI and then edited by a radiation oncologist; this step has repercussions on the adequacy the MRI-based syCT plan calculation, as each organ is assigned an average ED; therefore, the correctness of the target contour and the OAR identification as well as the choice of the significant number of

TABLE 6   Absolute difference of target and OARs DVH dosimetric parameters of the original CT and of the reworked CT vs. the corresponding syCT plans.

		PTV1		PTV2		PTV3		Colon		Body	
		Original	Reworked	Original	Reworked	Original	Reworked	Original	Reworked	Original	Reworked
Rectum Case 1	ΔV_{Dpre} (%)	14.83	0.49	9.12	0.23	8.05	0.06	-	-	-	-
	ΔD_{20cc} (Gy)	-	-	-	-	-	-	0.69	0.08	-	-
	γ (3%/3 mm) (%)	89.98	99.05	93.7	99.03	87.59	99.04	97.91	98.34	97.87	99.32
	γ(2%/2 mm) (%)	51.71	78.85	58.66	78.12	41.76	78.52	89.33	89.93	87.34	94.84
Rectum Case 2	ΔV_{Dpre} (%)	20.99	0.25	5.95	0.42	23.85	0.52	–	–	–	–
	$\Delta D_{0.5cc}$ (%)	–	–	–	–	–	–	3.94	0.03	–	–
	γ (3%/3 mm) (%)	79.88	99.64	93.9	99.6	77.32	98.14	82.42	89.10	95.51	99.28
	γ (2%/2 mm) (%)	44.04	83.95	68.87	87.38	40.01	84.05	68.48	78.08	85.31	94.95

OARs not reported in the table presented CT vs. syCT absolute difference of DVHs dosimetric parameters< 1 Gy or 1.5%, and a gamma analysis with 3%/3 mm and 2%/2 mm > 99.0% and 95.0%, respectively.

TABLE 7 Absolute difference of target DVH dosimetric parameters between CT and syCT, before and after plan reworking.
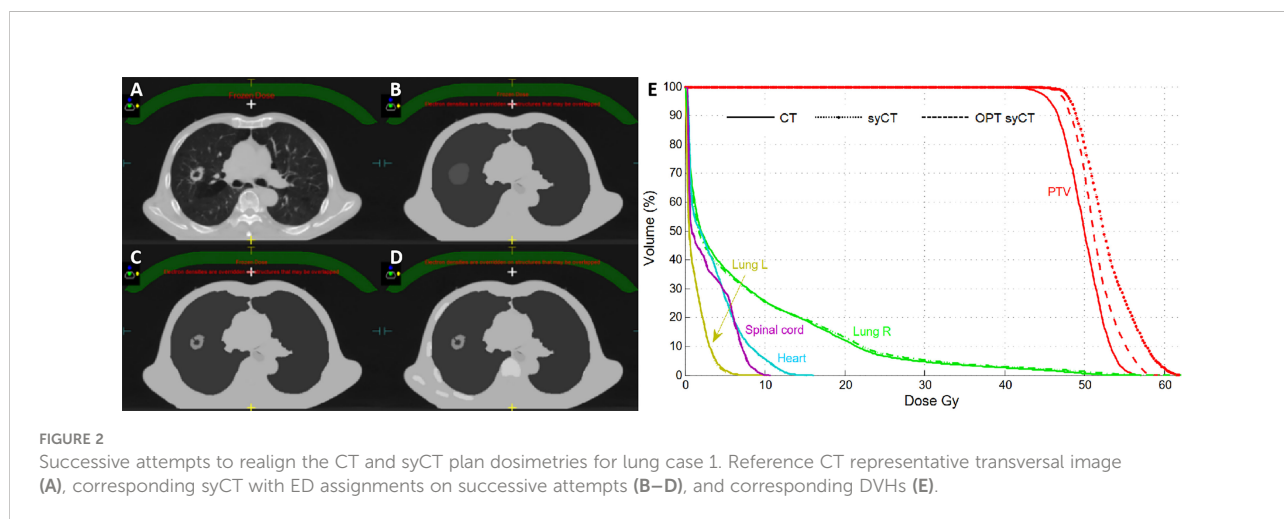
Parameter		PTV		Body	
		Original	Reworked	Original	Reworked
Brain Case	ΔV_{Dpre} (%)	20.22	1.08	–	-
	γ (3%/3 mm) (%)	97.23	99.90	99.68	99.90
	γ (2%/2 mm) (%)	69.87	96.07	94.77	97.64
Liver case 1	ΔV_{Dpre} (%)	8.32	1.30	-	-
	γ (3%/3 mm) (%)	75.37	99.84	97.26	99.66
	γ (2%/2 mm) (%)	33.51	94.68	92.39	98.33
Liver case 2	ΔV_{Dpre} (%)	4.72	0.5	–	–
	γ (3%/3 mm) (%)	81.97	99.74	97.06	99.53
	γ (2%/2 mm) (%)	60.71	94.31	89.53	96.88

OARs were not reported in the table because they presented CT vs. syCT absolute difference of DVHs dosimetric parameters< 1 Gy or 1.5%, and a gamma analysis with 3%/3 mm and 2%/2 mm > 99.0% and 95.0%, respectively.

contours are of paramount importance. Regarding the adjustment of OARs, if the constraints are related to the maximum dose, although it might seem reasonable to touch up only the part of the organ adjacent to the target, because the organ has its own density, then it is necessary for the accuracy of the calculation to edit it in full. Similarly, the ribs, which for most treatments are not drawn, in the case of recalculation on the syCT, are necessary to outline at least those that intersect the beams entry. Auto-segmentation could be a feasible solution to automatically contour targets and OARs during the online adaptive phase (55). Furthermore, considering that the calculation on the syCT is governed not only by the shape of the drawn organs but also by their average ED, it must be ensured that the priority of one organ over the other in case of their overlapping has been correctly assigned and that, in any case in the chain of successive steps, there has not been a "disturbing element" that could have influenced the final dose delivered. Organs with different densities can be an issue for the calculation accuracy; consequently, it would therefore be completely inappropriate to force a target to have an average ED if it includes parts with different densities.

The use of our procedure within the clinical workflow could be seen as an additional control to be included in the quality assurance of the treatment. Considering the sensitivity of the system to inhomogeneities, the organs that may have different densities within them (air bubbles in the case of the intestine, PTV including different tissues) must be properly managed within a clinical workflow; moreover, we must consider that the manual modification of the contours must anyway be done in a reasonable time. Whenever the MRI scan acquired at simulation would be used as imaging for the reference plan, the procedure proposed may also be useful; in this case, the transport of the contours between MR images (simulation to daily MR) should be more accurate, even if we cannot avoid their verification/editing if deemed necessary (48). Moreover, this process could be carried out off-line before the patient's treatment begins and would therefore have robustness comparable to the recalculation on the planning CT.
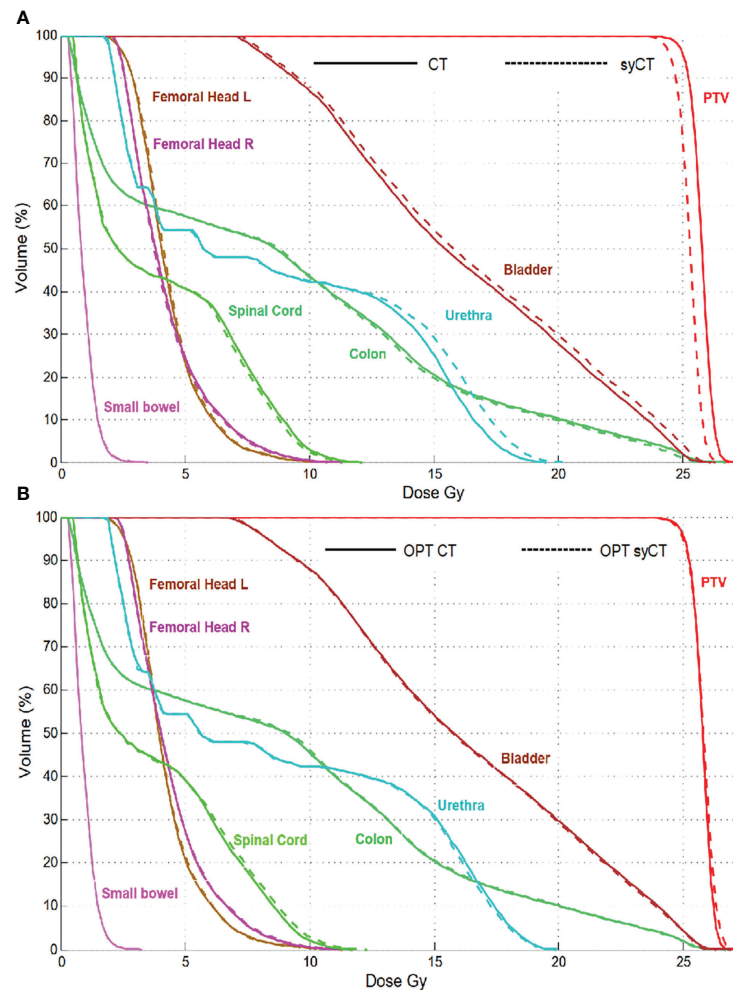

FIGURE 2
Successive attempts to realign the CT and syCT plan dosimetries for lung case 1. Reference CT representative transversal image **(A)**, corresponding syCT with ED assignments on successive attempts **(B–D)**, and corresponding DVHs **(E)**.

FIGURE 3
Rectum case 1: DVH comparison of the original CT plan and its corresponding syCT plan **(A)** and of the reworked CT reference plan with its corresponding syCT **(B)**.
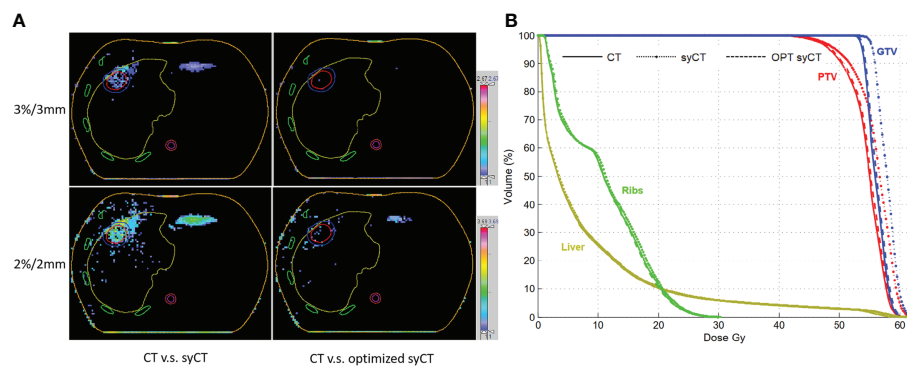

FIGURE 4
The gamma analysis among CT, syCT, and optimized syCT with criteria of 3%/3 mm and 2%/2 mm, respectively **(A)**; the comparison of DVH among CT, syCT, and optimized syCT **(B)**.

Among the limitations of this procedure is the fact that it only allows the estimation of the minimum error introduced by the bulk density assignment–based syCT. This therefore does not exclude unmanageable errors during the online process, as not accurate or exhaustive recontouring of OARs and all regions supposed to have different ED. Furthermore, high-density parts of a pps within the treatment field can affect dosimetry. In fact, no matter how accurately the patient may be positioned, small movements of the patient within the thermoplastic mask are always possible. Even if the parts of the pps in question were contoured during the treatment plan, the MRI would not be able to visualise them during treatment, and therefore, we would not be able to adjust for small differences as we do with contours. The recalculation on the online procedure would unfortunately not take this into account.

Conclusion

The accuracy of the reference treatment plan calculation on a SyCT can be influenced by several factors in the different steps of the clinical workflow of the Unity MR-Linac. The evaluation of the accuracy of its calculation can be easily inserted in the radiotherapy routine of the individual patient to highlight and correct in time the errors that may occur and to provide the RO with guidance on proceeding with treatment using either ATS or ATP.

Data availability statement

The raw data supporting the conclusions of this article will be made available by the authors, without undue reservation.

Ethics statement

The studies involving human participants were reviewed and approved by Ethics Committee of Sichuan Cancer Hospital, Sichuan Cancer Hospital. The patients/participants provided their written informed consent to participate in this study.

Author contributions

Conceptualization: BT and LO. Data acquisition: ML, PD, FW, XL, XF, and XY. Data analysis: ML, BW, FW, XF, and QH. Project administration: JL. Writing—original draft: BT and LO. Supervision: JL, LO, BT, and QH. Writing—review and editing: BT, BW, PD, FW, and XY. All authors contributed to the article and approved the submitted version.

Funding

Acknowledgments

Conflict of interest

The authors declare that the research was conducted in the absence of any commercial or financial relationships that could be construed as a potential conflict of interest.

Publisher's note

All claims expressed in this article are solely those of the authors and do not necessarily represent those of their affiliated organizations, or those of the publisher, the editors and the reviewers. Any product that may be evaluated in this article, or claim that may be made by its manufacturer, is not guaranteed or endorsed by the publisher.

References

1. Pathmanathan AU, Van As N, Kerkmeijer L, Christodouleas J, Caf L, Vesprini D, et al. Magnetic resonance imaging-guided adaptive radiation therapy: A "Game changer" for prostate treatment? *Int J Radiat Oncol Biol Phys* (2018) 100(2):361. doi: 10.1016/j.ijrobp.2017.10.020

2. Stemkens B, Glitzner M, Kontaxis C, Denis de Senneville B, Stemkens Prins FM, Crijns P, et al. Effect of intra-fraction motion on the accumulated dose for free-breathing MR-guided stereotactic body radiation therapy of renal-cell carcinoma. *Phys Med Biol* (2017) 62(18):7407. doi: 10.1088/1361-6560/aa83f7

3. Kleijnen JPJE, Van Asselen B, Burbach JPM, Intven M, Philippens MEP, Reerink O, et al. Evolution of motion uncertainty in rectal cancer: implications

for adaptive radiotherapy. *Phys Med Biol* (2015) 61(1):1. doi: 10.1088/0031-9155/61/1/1

4. Chin S, Eccles CL, McWilliam A, Chuter R, Walker E, Whitehurst P, et al. Magnetic resonance-guided radiation therapy: a review. *J Med Imaging Radiat Oncol* (2020) 64(1):163–77. doi: 10.1111/1754-9485.12968

5. Winkel D, Bol GH, Kroon PS, Asselen BV, Hackett SS, Werensteijn-Honingh AM, et al. Adaptive radiotherapy: The elekta unity MR-linac concept. *Clin Trans Radiat Oncol* (2019) 18:54–59. doi: 10.1016/j.ctro.2019.04.001

6. Chamberlain M, Krayenbuehl J, Timmeren J, Wilke L, Balermpas P. Head and neck radiotherapy on the MR linac: a multicenter planning challenge amongst

MRIdian platform users. *Strahlenther Und Onkol* (2021),197(12): 1093–1103. doi: 10.1007/s00066-021-01771-8

7. Boldrini L, Piras A, Chiloiro G, Autorino R, Gambacorta MA. Low Tesla magnetic resonance guided radiotherapy for locally advanced cervical cancer: first clinical experience. *Tumori* (2020) 106(6):497–505. doi: 10.1177/0300891620901752

8. Gani C, Boeke S, Mcnair H, Ehlers J, Zips D. Marker-less online MR-guided stereotactic body radiotherapy of liver metastases at a 1.5 T MR-linac – feasibility, workflow data and patient acceptance. *Clin Trans Radiat Oncol* (2021) 26:55–61. doi: 10.1016/j.ctro.2020.11.014

9. Lorenzo P, Romano A, Chiloiro G, Davide C. B luca and c G Francesco, mattiucci Vincenzo, valentini: On-line adaptive MR guided radiotherapy for locally advanced pancreatic cancer: Clinical and dosimetric considerations. *Tech Innov Patient Support Radiat Oncol* (2020) 15:15–21. doi: 10.1016/j.tipsro.2020.06.001

10. Gupta A, Dunlop A, Mitchell A, Nill DMS, Barnes H, Newbold K, et al. Online adaptive radiotherapy for head and neck cancers on the MR linear accelerator: Introducing a novel modified adapt-to-Shape approach. (2022) 10 (32):48–51. doi: 10.1016/j.ctro.2021.11.001

11. Marcel VH, Alan MW, Michael D, Corinne FF, Ananya C. Magnetic resonance imaging-guided radiation therapy: A short strengths, weaknesses, opportunities, and threats analysis. *Int J Radiat Oncol Biol Phys* (2018) 101 (5):1057–60. doi: 10.1016/j.ijrobp.2017.11.009

12. Dowling JA, Sun J, Pichler P, Rivest-Henault D, Ghose S, Richardson H, et al. Automatic substitute computed tomography generation and contouring for magnetic resonance imaging (MRI)-alone external beam radiation therapy from standard MRI sequences. *Int J Radiat Oncol Biol Phys* (2015) 93(5):1144–53. doi: 10.1016/j.ijrobp.2015.08.045

13. Johansson A, Karlsson M, Nyholm T. CT substitute derived from MRI sequences with ultrashort echo time. *Med Phys* (2011) 38(5):2708–14. doi: 10.1118/1.3578928

14. Hsu SH, Cao Y, Huang K, Feng M, Balter JM. Investigation of a method for generating synthetic CT models from MRI scans of the head and neck for radiation therapy. *Phys Med Biol* (2013) 58(23):8419–35. doi: 10.1088/0031-9155/58/23/8419

15. Wang C, Chao M, Lee L, Xing L. MRI-Based treatment planning with electron density information mapped from CT images: a preliminary study. *Technol Cancer Res Treat* (2008) 7(5):341. doi: 10.1177/153303460800700501

16. Lambert J, Greer PB, Menk F, Patterson J, Parker J, Dahl K, et al. MRI-Guided prostate radiation therapy planning: Investigation of dosimetric accuracy of MRI-based dose planning. *Radiother Oncol J Eur Soc Ther Radiol Oncol* (2011) 98(3):330–4. doi: 10.1016/j.radonc.2011.01.012

17. Stanescu T, Jans HS, Pervez N, Stavrev P, Fallone BG. A study on the magnetic resonance imaging (MRI)-based radiation treatment planning of intracranial lesions. *Phys Med Biol* (2008) 53(13):3579–93. doi: 10.1088/0031-9155/53/13/013

18. Jonsson JH, Karlsson MG, Karlsson M, Nyholm T. Treatment planning using MRI data: an analysis of the dose calculation accuracy for different treatment regions. *Radiat Oncol* (2010) 5(1):62. doi: 10.1186/1748-717X-5-62

19. Kristensen BH, Laursen FJR, LøGager V, Geertsen PF, Krarup-Hansen A. Dosimetric and geometric evaluation of an open low-field magnetic resonance simulator for radiotherapy treatment planning of brain tumours. *Radiother Oncol* (2008) 87(1):100–9. doi: 10.1016/j.radonc.2008.01.014

20. Siversson C, Nordstrom F, Nilsson T, Nyholm T, Jonsson J, Gunnlaugsson A, et al. Technical note: MRI only prostate radiotherapy planning using the statistical decomposition algorithm. *Med Phys* (2015) 42(10):6090–7. doi: 10.1118/1.4931417

21. Demol B, Boydev C, Korhonen J, Reynaert N. Dosimetric characterization of MRI-only treatment planning for brain tumors in atlas-based pseudo-CT images generated from standard T1-weighted MR images. *Med Phys* (2016) 43(12): 6557–68. doi: 10.1118/1.4967480

22. Dowling JA, Lambert J, Parker J, Salvado O, Fripp J, Capp A, et al. An atlas-based electron density mapping method for magnetic resonance imaging (MRI)-alone treatment planning and adaptive MRI-based prostate radiation therapy. *Int J Radiat Oncol Biol Phys* (2012) 83(1):e5–11. doi: 10.1016/j.ijrobp.2011.11.056

23. Kapanen M, Tenhunen M. T1/T2*-weighted MRI provides clinically relevant pseudo-CT density data for the pelvic bones in MRI-only based radiotherapy treatment planning. *Acta Oncol* (2013) 52(3):612–8. doi: 10.3109/0284186X.2012.692883

24. Jonsson JH, Akhtari MM, Karlsson MG, Johansson A, Asklund T, Nyholm T. Accuracy of inverse treatment planning on substitute CT images derived from MR data for brain lesions. *Radiat Oncol* (2015) 10:13. doi: 10.1186/s13014-014-0308-1

25. Yu H, Caldwell C, Balogh J, Mah K. Toward magnetic resonance-only simulation: segmentation of bone in MR for radiation therapy verification of the head. *Int J Radiat Oncol Biol Phys* (2014) 89(3):649–57. doi: 10.1016/j.ijrobp.2014.03.028

26. Gudur MS, Hara W, Le QT, Wang L, Xing L, Li R. A unifying probabilistic Bayesian approach to derive electron density from MRI for radiation therapy treatment planning. *Phys Med Biol* (2014) 59(21):6595–606. doi: 10.1088/0031-9155/59/21/6595

27. Catana C, Van D, Benner T, Michel CJ, Hamm M, Fenchel M, et al. Toward implementing an MRI-based PET attenuation-correction method for neurologic studies on the MR-PET brain prototype. *J Nucl Med Off Publ Soc Nucl Med* (2010) 51(9):1431. doi: 10.2967/jnumed.109.069112

28. Hsu S, Dupre P, Peng Q, Tomé WA. A technique to generate synthetic CT from MRI for abdominal radiotherapy. *J Appl Clin Med Phys* (2020) 21(2):136–43. doi: 10.1002/acm2.12816

29. Tang B, Wu F, Fu Y, Wang X, Hou Q. Dosimetric evaluation of synthetic CT image generated using a neural network for MR-only brain radiotherapy. *J Appl Clin Med Phys* (2021) 22(3): 55–62. doi: 10.1002/acm2.13176

30. Uh J, Merchant TE, Li Y, Li X, Hua C. MRI-Based treatment planning with pseudo CT generated through atlas registration. *Med Phys* (2013) 41(5):051711. doi: 10.1118/1.4873315

31. Edmund JM, Nyholm T. A review of substitute CT generation for MRI-only radiation therapy. *Radiat Oncol* (2017) 12(1):28. doi: 10.1186/s13014-016-0747-y

32. Han X. MR-based synthetic CT generation using a deep convolutional neural network method. *Med Phys* (2017) 44(4):1408–19. doi: 10.1002/mp.12155

33. Kazemifar S, McGuire S, Timmerman R, Wardak Z, Nguyen D, Park Y, et al. MRI-Only brain radiotherapy: Assessing the dosimetric accuracy of synthetic CT images generated using a deep learning approach. *Radiother Oncol* (2019) 136:56–63. doi: 10.1016/j.radonc.2019.03.026

34. Lei Y, Harms J, Wang T, Liu Y, Liu T. MRI Only based synthetic CT generation using dense cycle consistent generative adversarial networks. *Med Phys* (2019) 48(6):3565–81. doi: 10.1002/mp.13617

35. Liu F, Yadav P, Baschnagel AM, McMillan AB. MR-based treatment planning in radiation therapy using a deep learning approach. *J Appl Clin Med Phys* (2019) 20(3):105–14. doi: 10.1002/acm2.12554

36. Maspero M, Bentvelzen LG, Savenije MH, Guerreiro F, Seravalli E, Janssens GO, et al. Deep learning-based synthetic CT generation for paediatric brain MR-only photon and proton radiotherapy. *Radiother Oncol* (2020) 153:197–204. doi: 10.1016/j.radonc.2020.09.029

37. Yoo GS, Luu HM, Kim H, Park W, Pyo H, Han Y, et al. Feasibility of synthetic computed tomography images generated from magnetic resonance imaging scans using various deep learning methods in the planning of radiation therapy for prostate cancer. *Cancers (Basel)* (2021) 14(1):1–13. doi: 10.3390/cancers14010040

38. Cusumano D, Lenkowicz J, Votta C, Boldrini L, Placidi L, Catucci F, et al. A deep learning approach to generate synthetic CT in low field MR-guided adaptive radiotherapy for abdominal and pelvic cases. *Radiother Oncol* (2020) 153:205–12. doi: 10.1016/j.radonc.2020.10.018

39. Chen S, Qin A, Zhou D, Yan D. Technical note: U-net generated synthetic CT images for magnetic resonance imaging-only prostate intensity-modulated radiation therapy treatment planning. *Med Phys* (2018). doi: 10.1002/mp.13247

40. Peter K, Ilyes B, Sadegh R, Jue J, Margie H, Deasy JO, et al. Patch-based generative adversarial neural network models for head and neck MR-only planning. *Med Phys* (2020) 47(2):626–42. doi: 10.1002/mp.13927

41. Chen L, Price RA, Lu W, Li J, Qin L, Mcneeley S, et al. MRI-Based treatment planning for radiotherapy: Dosimetric verification for prostate IMRT. *Int J Radiat Oncol Biol Phys* (2004) 60(2):636–47. doi: 10.1016/j.ijrobp.2004.05.068

42. Doemer A, Chetty IJ, Glide-Hurst C, Nurushev T, Hearshen D, Pantelic M, et al. Evaluating organ delineation, dose calculation and daily localization in an open-MRI simulation workflow for prostate cancer patients. *Radiat Oncol* (2015) 10(1):37. doi: 10.1186/s13014-014-0309-0

43. Kirkby C, Murray B, Rathee S, Fallone BG. Lung dosimetry in a linac-MRI radiotherapy unit with a longitudinal magnetic field. *Med Phys* (2010) 37(9):4722–32. doi: 10.1118/1.3475942

44. Kirkby C, Stanescu T, Rathee S, Carlone M, Murray B, Fallone BG. Patient dosimetry for hybrid MRI-radiotherapy systems. *Med Phys* (2008) 35(3):1019–27. doi: 10.1118/1.2839104

45. Cacicedo J, Navarro-Martin A, Gonzalez-Larragan S, Bari BD, Dahele M. Systematic review of educational interventions to improve contouring in radiotherapy. *Radiother Oncol* (2019) 144:86–92. doi: 10.1016/j.radonc.2019.11.004

46. Belkacemi Y, Colson-Durand L, Fayolle-Campana M, Pons P, Rialland A, Bastuji-Garin S, et al. A "Wake-up call" for routine morbidity and mortality review meetings procedure as part of a quality governance program in radiotherapy departments: Results of the proust survey. *Pract Radiat Oncol* (2018) 9(2):108–14. doi: 10.1016/j.prro.2018.09.004

47. Cusumano D, Placidi L, Teodoli S, Boldrini L, Azario L. On the accuracy of bulk synthetic CT for MR-guided online adaptive radiotherapy. *La Radiol Med* (2019) 125(2):157–64. doi: 10.1007/s11547-019-01090-0

48. Tyagi N, Zelefsky MJ, Wibmer A, Zakian K, Hunt M. Clinical experience and workflow challenges with magnetic resonance-only radiation therapy simulation and planning for prostate cancer. *Phys Imaging Radiat Oncol* (2020) 16:43–9. doi: 10.1016/j.phro.2020.09.009

49. Thorwarth D, Low DA. Technical challenges of real-time adaptive MR-guided radiotherapy. *Front Oncol* (2021) 11:634507. doi: 10.3389/fonc.2021.634507

50. Mannerberg A, Persson E, Jonsson J, Gustafsson CJ, Ceberg S. Dosimetric effects of adaptive prostate cancer radiotherapy in an MR-linac workflow. *Radiat Oncol* (2020) 15(1):168–77. doi: 10.1186/s13014-020-01604-5

51. Raaymakers BW, Jürgenliemk-Schulz I, Bol GH, Glitzner M, Kotte A, Asselen BV, et al. First patients treated with a 1.5 T MRI-linac: clinical proof of concept of a high-precision, high-field MRI guided radiotherapy treatment. *Phys Med Biol* (2017) 62(23):L41–50.doi: 10.1088/1361-6560/aa9517

52. Bertelsen AS, Schytte T, Møller PK, Mahmood F, Bernchou U. First clinical experiences with a high field 1.5 T MR linac. *Acta Oncol* (2019),58(10):1352–7. doi: 10.1080/0284186X.2019.1627417

53. Bonomo P, Russo ML, Nachbar M, Boeke S, Gani C. 1.5 T MR-linac planning study to compare two different strategies of rectal boost irradiation. *Clin Trans Radiat Oncol* (2021) 26:86–91. doi: 10.1016/j.ctro.2020.11.016

54. Jaffray DA, Carlone MC, Milosevic MF, Breen SL, Stanescu T, Rink A, et al. A facility for magnetic resonance–guided radiation therapy. *Semin Radiat Oncol* (2014) 24(3):193–5. doi: 10.1016/j.semradonc.2014.02.012

55. Yun J, Yip E, Gabos Z, Wachowicz K, Rathee S, Fallone BG. Neural-network based autocontouring algorithm for intrafractional lung-tumor tracking using linac-MR. *Med Phys* (2015) 42(5):2296–310. doi: 10.1118/1.4916657